

## CONTROLLED SYNTHESIS OF GD-DOPED SUPERPARAMAGNETIC IRON OXIDE NANOPARTICLES TOWARDS STABLE AND BIOCOMPATIBLE CONTRAST AGENT

Kateřina POLÁKOVÁ, Zdeňka MEDŘÍKOVÁ, Ondřej MALINA, Klára ČÉPE, Radek ZBOŘIL

*Regional Centre of Advanced Technologies and Materials, Palacký University in Olomouc, Olomouc, Czech Republic, EU, [katerina.polakova@upol.cz](mailto:katerina.polakova@upol.cz)*

### Abstract

Superparamagnetic iron oxides (SPIO) nanoparticles (NPs) are used as negative contrast agents in magnetic resonance imaging (MRI). However, controlled synthesis of highly stable, biocompatible, reproducible SPIO NPs in mild conditions is still very rare which is demonstrated by the fact that many commercial contrast agents have been withdrawn from the market due to the problems with effective and reproducible synthesis. Here, we introduce a facile and controlled synthesis of Gd-doped SPIO NPs. We have found that different amount of Gadolinium (5, 10 and 20 %) replacing the Fe mols in the beginning of the synthesis influence the final physico-chemical properties of the later products. With increasing amount of Gd ions, the higher amount of organic versus inorganic content is calculated (from TGA analysis) which is mirrored in decreasing of saturation magnetization (from 78 Am<sup>2</sup>/kg for SPIO without Gd to 15 Am<sup>2</sup>/Kg for 20 % Gd-doped SPIO). All prepared samples are stable in PBS and till 10 % of Gd doping biocompatible at high concentrations used (500 µg/ml). Moreover, 10 % Gd-SPIO (cMNPs\_Gd10) shows the most stable properties also in a high ionic strength (1 M of NaCl). This sample is promising for mesenchymal stem cells (MSC) labeling. After 24 hours, robust internalization into the MSC was confirmed by fluorescence optical microscopy and by strong negative signal of SPIO labeled MSC measured by clinical 1.5 T MRI.

**Keywords:** Controlled synthesis, superparamagnetic iron oxides (SPIO), in vitro characterization, mesenchymal stem cells (MSC), magnetic resonance imaging (MRI)

## 1. MATERIALS AND METHODS

### 1.1. Materials

Carboxymethylcellulose, sodium salt (CMC), iron (II) sulphate heptahydrate (FeSO<sub>4</sub>·7H<sub>2</sub>O), gadolinium (III) chloride (GdCl<sub>3</sub>·6H<sub>2</sub>O), N-(3-dimethylaminopropyl)-N'-ethylcarbodiimide hydrochloride (EDC) were from Sigma Aldrich (Germany) in analytical grade. Sodium hydroxide (p.a.), 99.8 % acetic acid, 37 % HCl, 28 % NH<sub>4</sub>OH (p.a.), NaCl (p.a.) were obtained from P-LAB (Czech Republic). Alexa Fluor 488 Hydrazide (AlexaFluo) was obtained from Life Technologies, Czech Republic. All chemicals were used without further purification. For all experiments double, distilled water (ddH<sub>2</sub>O) was used.

### 1.2. Preparation of carboxylated MNPs (cMNPs) and Gd-doped cMNPs (cMNPs\_Gd)

Magnetite NPs stabilized by CMC (cMNPs) were prepared according to a protocol described earlier by Medříková et al. [1]. Briefly, CMC (1 g) was dissolved in ddH<sub>2</sub>O (30 mL) and heated up to 303 K. FeSO<sub>4</sub>·7H<sub>2</sub>O (720 mg) was dissolved in ddH<sub>2</sub>O (10 mL), pre-acidified by 37 % HCl (total volume of 100 µL) and added to CMC solution under mechanical stirring (300 rpm). NH<sub>4</sub>OH (28 %, 7 mL) was added to the mixture. Over a period of 15 min, the temperature was raised to 323 K followed by addition of 28 % NH<sub>4</sub>OH (5 mL). After another 15 min, the reaction mixture was removed from the hot plate and the formed magnetic colloid was immediately centrifuged (20,000 g, 293 K) for 1 h. The magnetic pellet was resuspended in 60 mL ddH<sub>2</sub>O and sonicated for 15 min. Subsequently, it was again centrifuged (20,000 g, 293 K, 1 h), the pellet resuspended in ddH<sub>2</sub>O (40 mL) and sonicated.

Carboxylated Gd-doped MNPs (cMNPs\_Gd) were prepared according the same protocol as cMNPs including replacing 5 %, 10 % or 20 % mols of Fe in the reaction mixture by the same amount of Gd mols. The prepared magnetic nanoparticles were marked cMNPs\_Gd5, cMNPs\_Gd10, and cMNPs\_Gd20, respectively. Briefly, mixtures consisting of 0.684 g of FeSO<sub>4</sub>·7H<sub>2</sub>O and 0.048 g of GdCl<sub>3</sub>·6H<sub>2</sub>O (cMNPs\_Gd5), 0.648 g of FeSO<sub>4</sub>·7H<sub>2</sub>O and 0.096 g of GdCl<sub>3</sub>·6H<sub>2</sub>O (cMNPs\_Gd10), and 0.576 g of FeSO<sub>4</sub>·7H<sub>2</sub>O and 0.193 g of GdCl<sub>3</sub>·6H<sub>2</sub>O (cMNPs\_Gd20) were used instead of 0.72 g of FeSO<sub>4</sub>·7H<sub>2</sub>O in the protocol for the preparation of Gd-doped cMNPs.

The final magnetic colloids were centrifuged (1,000 g, 298 K) for 20 min to remove any aggregates. The supernatants containing carboxylated magnetic nanoparticles (cMNPs) or Gd-doped cMNPs were collected and stored at 4 °C.

### 1.3. Determination of stability

The stability of prepared magnetic nanoparticles (NPs) was tested in phosphate buffered saline (PBS) consisting of 0.05 M phosphate buffer (pH 7.4) and 0.15 M NaCl solution (final concentrations). For each experiment, 250 µL of NPs (1 g of Fe<sub>3</sub>O<sub>4</sub>/L) were taken into 0.5 mL of phosphate buffered saline (0.1 M phosphate buffer, 0.3 M NaCl, pH 7.4) adjusted to 1 mL by ddH<sub>2</sub>O. The testing tubes were incubated at 310 K and at shaking speed 150 rpm. The hydrodynamic diameters of NPs ( $d_H$ ) were determined before and after 24 hours of its incubation in PBS. The gadolinium release from NPs was determined after 24 hours of its incubation in PBS. The non-released and released Gd was determined in pellets and supernatants, respectively, after centrifugation (20 000 g, 30 min) by ICP-MS.

### 1.4. Preparation of AlexaFluo modified cMNPs or cMNPs-Gd10

Immobilizations of fluorescent mark onto NPs surface were carried out with the activations of carboxyl groups of NPs via EDC chemistry. In brief, 50 µL of EDC (1 mg) were added to 1 mL of NPs (1 g of Fe<sub>3</sub>O<sub>4</sub>/L) and the activation was performed for 30 min. Then, 0.03 mg of AlexaFluo was added and the immobilization was performed for 16 h, at 150 rpm, 10 °C, and in the dark. Unbounded agents were removed by centrifugation.

### 1.5. Techniques for physicochemical characterization

Microscopic images were obtained by transmission electron microscopy (TEM) JEM2100 microscope operated at 200 kV with a point-to-point resolution of 1.9 Å and high-resolution transmission electron microscopy (HRTEM) TITAN 60-300kV, operating at 300 kV. STEM - Energy Dispersive X-ray Spectroscopy (EDS) with acquisition time 20 min was used for chemical mapping. Thermogravimetric analysis was performed by a thermal analyzer STA 449 C Jupiter (Netzsch Instrument). Hydrodynamic diameter ( $d_h$ ) and zeta potential values ( $\zeta$ ) of cMNPs were determined by Dynamic Light Scattering (DLS) method using the instrument Malvern Zetasizer Nano (Malvern Instruments Ltd., Worcestershire, UK). The iron content in the solution was determined with a protocol of the ferrozine assay. The gadolinium concentration was determined by ICP-MS.

A superconducting quantum interference device (SQUID, MPMS XL-7, Quantum Design, U.S.A.) was employed for the magnetization measurements. The hysteresis loop of the studied sample was collected at a temperature of 300 K in external magnetic fields ranging from - 5 to + 5 T. The magnetization values were corrected assuming the response of the sample holder and respective Pascal constants.

### 1.6. In vitro cytotoxicity

The viability of NIH/3T3 cells (ATCC, USA) was determined with using the 3-(4,5-dimethylthiazol-2-yl)-2,5-diphenyltetrazolium bromide (MTT) assay (Sigma Aldrich). Cells were seeded in a 96-well plate (TPP, Biotech). After spreading (24h), cells were incubated with different concentration of various cMNPs nanoparticles in a fully-humidified incubator. After treatment with cMNPs (24 h), 20 µl of an MTT solution (concentration

of 5 mg/ml) was added into the each well. After incubation (4 h), the MTT solution was gently removed and dimethylsulfoxide (100 µl) was added to dissolve formazan crystals. Absorbance was measured at 570 nm using an Infinite PRO M200 multiplate reader (Tecan, Austria). Results are presented in relative viability with respect of control untreated cells.

### 1.7. Stem cell labeling and MRI

hMSCs were isolated from the fatty tissue of three healthy donors who had undergone cosmetic liposuction (one male, two female). Isolation of hMSCs was based on the incubation of lipoaspirates with collagenase. MSCs were expanded in complete DMEM supplemented with 5 % platelet lysate. All animal experiments were performed in accordance with the law of Czech Republic (Law on Animal Protection and Decree of Ministry of Agriculture on Experimental Animal Use and Breeding) and were approved by the Committees for the Use of Experimental Animals at Masaryk University and Palacký University. All collection of waste lipoaspirates from liposuction was performed after approval of the Ethical Committee of Masaryk University and with signature-documented informed consent of patients.

For cellular internalization of cMNPs particles labeled by AlexaFluo and visual microscopic quantification of viable labeled cells Olympus IX 70 light fluorescence microscopes (Olympus Corporation) was used. The cells were grown on 24 well-plate. After spreading of cells (24hours), 100 µg/ml of cMNP\_Gd10 conjugated with fluorescein dye was added and imaged after 4 hours, 1day and 5 days.

For MRI phantom study of labeled cells, cells were grown on 24well plate. After 24 hours, 100µg/ml of cMNPs\_Gd10 particles were added into each well and incubated overnight. After that, medium was removed, adhered cells were trypsinized, detached from surface and centrifugated. The obtained pellet (500 thousand cells) was fixed in 1 % agar in 1.5ml eppendorf tube. The eppendorf with pellet containing labeled cells was measured on 1.5 T MRI clinical magnet using Sag T2 FrFSE sequences (TR:2600, TE:90, matrix 2X2)

## 2. INTRODUCTION

Magnetic resonance imaging (MRI) has become a powerful technique in the clinical diagnosis of disease and in animal imaging. MRI enables images of living subjects with high spatial resolution and no penetration limit only by using of external magnetic field on tissue water protons [2-4]. To increase a diagnostic accuracy and most recently for molecular targeting or stem cell monitoring superparamagnetic iron oxide nanoparticles (SPIO) and paramagnetic chelates are being used as negative and positive contrast agents [5-7]. SPIO NPs are consisted of maghemite ( $\gamma$ -Fe<sub>2</sub>O<sub>3</sub>) or magnetite (Fe<sub>3</sub>O<sub>4</sub>) spinel structure having two nonequivalent magnetic sublattices revealing very high magnetic susceptibility. Moreover, below a critical size (usually below 100 nm) superparamagnetic behavior occurs. This means that SPIO NPs show higher saturation magnetization than bulk material of the same chemical structure when using magnetic field, on the other hand, after switching off the external magnetic field the magnetization become zero and without remanence and coercivity. Therefore, during MR investigation SPIO can react very fast on MR magnetic field, causing a decrease of relaxation times of surrounding water protons which gives the negative signal of imaged tissue in T2-weighted images [8,9]. SPIO NPs of various sizes and polymer coatings has been clinically tested for imaging of bowel and abdomen (Lumirem, Abdoscan) [10,11], liver/spleen (Endorem, Feridex, Resovist), lymph node imaging (AMI-227 - Sinerem and Combidex), bone marrow imaging (AMI-227), perfusion imaging (NC100150 - Clariscan) or MR angiography (NC100150) [12] or cellular imaging [13].

However, almost all commercial contrast agents have been recently withdrawn from the market mainly due to the problems with effective and reproducible synthesis. Most of SPIO have been synthesized by coprecipitation of iron salts which leads to nonuniform particles with non-perfectly defined magnetic properties. Reproducibility is thus also difficult. Other types of synthetic procedures include microemulsion, hydro-thermal or thermal

decomposition [14,15]. Generally, these syntheses are expensive with low quantities or hardly reproducible therefore the product in the clinics would be very expensive. Procedures leading to controlled synthesis of highly stable, biocompatible, reproducible SPIO NPs of high quantities are still very rare.

Here, we demonstrate a facile and controlled synthesis of SPIO nanoparticles coated with carboxymethylcellulose which are biocompatible and very stable in PBS and also in a high ionic strength only by using appropriate amount of Gd chelated in the carboxymethylcellulose polymer (CMC). SPIO sample with 10 % of Gd doped CMC shows promising results in mesenchymal stem cell imaging as negative MR contrast agent.

### 3. RESULTS AND DISCUSSION

The carboxymethylcellulose stabilized MNPs (cMNPs) were synthesized by the aqueous precipitation approach described earlier [1]. The morphology and structural organization of as-prepared nanoparticles were observed by TEM (**Figure 1**). The TEM image of colloidal cMNPs (**Figure 1a**) shows that nanoparticles were arranged into superclusters (densely packed nanoparticles) as described in the previous study [1]. **Figures 1b-d** show impact of Gd doping on structural organization of cMNPs. The increasing Gd content in the reaction leads to the destruction of superclusters. Whereas superclusters were partially recognizable in cMNPs\_Gd5 (**Figure 1b**), the nanoparticles in samples cMNPs\_Gd10 and cMNPs\_Gd20 lacked supercluster arrangement (**Figure 1c** and **1d**, respectively).

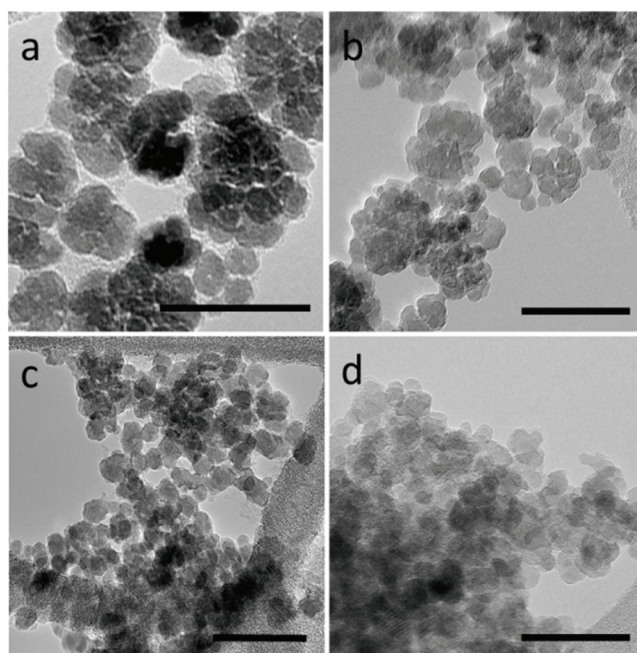


**Figure 1** TEM images of (a) cMNPs, (b) cMNPs\_Gd5, (c) cMNPs\_Gd10, and (d) cMNPs\_Gd20. Scale bar is 40 nm.

The accurate final contents of Gd in Gd-doped cMNPs (cMNPs\_Gd5, cMNPs\_Gd10, and cMNPs\_Gd20) were measured by ICP-MS (**Table 1**) and were found to be 0.156, 0.332, and 0.712 g of Gd per 1 g of Fe, respectively. These concentrations are fully comparable with Gd:Fe ratios used in the reaction mixtures. The inorganic (Gd and Fe<sub>2</sub>O<sub>3</sub>) and organic (polymer) contents were determined thermogravimetrically (**Table 1**) and ranged from 80.4 to 48.5 for inorganic and from 19.6 to 51.5 for organic compounds, respectively. The polymer content increases by increasing of Gd amount in the sample which suggested that Gd play a key role as crosslinker agent for CMC. Due to the presence of Gd during the preparation of nanoparticles the higher

amount of polymer is attached on the surface of nanoparticles. This effect is achieved by formation of complex between  $\text{Gd}^{3+}$  and carboxyl groups of CMC.

**Table 1** Physico-chemical characterization of cMNPs and Gd-doped cMNPs

Sample	Inorganic /organic content <sup>a</sup> (w/w %)	Magnetization (emu/g)	Gd content <sup>b</sup> (g/g Fe)	Gd content <sup>c</sup> (g/g Fe)
cMNPs	80.4/19.6	78.1	NA	NA
cMNPs-Gd5	62.5/37.5	37.5	$0.156 \pm 0.004$	$0.157 \pm 0.013$
cMNPs-Gd10	51.8/48.2	32.8	$0.332 \pm 0.008$	$0.325 \pm 0.011$
cMNPs-Gd20	48.5/51.5	15.2	$0.712 \pm 0.009$	$0.694 \pm 0.008$

<sup>a</sup> Determined thermogravimetrically

<sup>b</sup> Determined by ICP-MS

<sup>c</sup> Determined by ICP-MS after 24 hours exposure to PBS

In order to investigate magnetic properties of the prepared materials, hysteresis loops were measured at 300 K (see **Figure 2**). The saturation magnetization values of cMNPs and Gd-doped cMNPs, which ranged between 78.1 and 15.2, are listed in **Table 1**. These values are lower than that reported for bulk  $\text{Fe}_3\text{O}_4$  (saturation magnetization of 89 emu/g) [15]. The reduction in the saturation magnetization can be explained in terms of finite-size effects, presence of organic substance (having a diamagnetic nature), and in the case of Gd-doped cMNPs also presence of gadolinium complexed with carboxyl groups of the polymer (having a paramagnetic nature) contributes to lower values. In our case, the effects of organic substance and/or gadolinium chelated with organic substance are prevailing as the magnetization values are normalized to the weight content of the sample. Moreover, remanence and coercivity of all prepared materials are almost undetectable indicating that the cMNPs clusters and Gd-doped cMNPs possess superparamagnetic properties at room temperature.

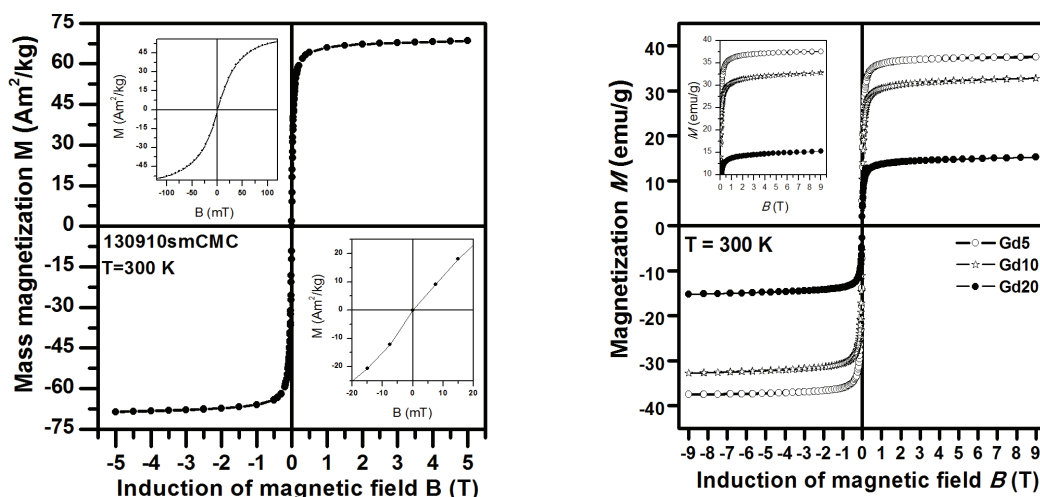


**Figure 2** Hysteresis loops of the synthesized cMNPs (left) and Gd-doped cMNPs (right) measured at a temperature of 300 K

The stability of Gd-doped cMNPs (in terms of Gd release from polymer) were investigated using their incubation in PBS for 24 hours. It was measured that a content of Gd did not decrease in all Gd-doped cMNPs. Simultaneously, Gd was not detected in supernatants which indicate high stability of bonding between gadolinium and carboxyl groups of CMC. The mean hydrodynamic diameters ( $d_h$ ) before and after exposure of nanoparticles to PBS (**Figure 3**) were determined by DLS measurements. The results indicate that the Gd doping led to increase in  $d_h$  values. However, Gd-doping did not decrease the stability of cMNPs because this increase of  $d_h$  values can be contributed to higher polymer content on the nanoparticles surface. This

statement is supported by further lowering of  $d_h$  of Gd-doped cMNPs after their 24h exposure to PBS which again indicate a high stability of all prepared nanoparticles. These decreases of  $d_h$  values could be a result of interaction between Na ions and carboxyl groups.

We further confirmed that Gd is chelated in polymer (CMC) corona by using chemical mapping (**Figure 4a**). Moreover, the higher stability of cMNPs\_Gd10 compared to bare cMNPs even at high ionic strength (**Figure 4b**) make this sample suitable and promising for in vivo bio-application. Results from viability measurements (**Figure 5**) show that only cMNPs\_Gd20 sample is significantly more toxic in concentrations above 350  $\mu\text{g/ml}$  (IC 50 about 500  $\mu\text{g/ml}$ ) probably due to the higher amount of Gd located on the outer shell of CMC. These Gd ions are thus in closer contact with the membrane of cells which can cause cytotoxicity. On the other hand, the rest three samples are biocompatible and viability of cells is not less than 80 % till concentration of 500  $\mu\text{g/ml}$ .

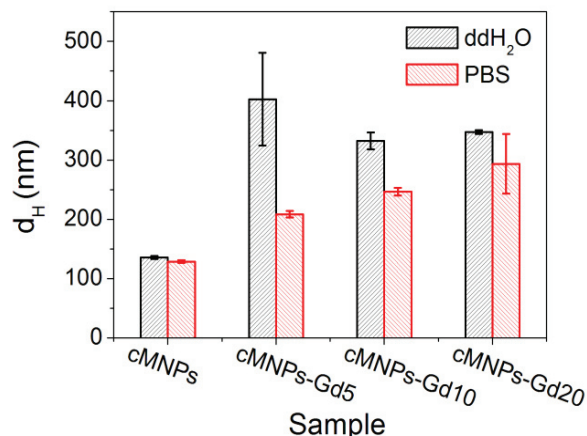


**Figure 3** The mean hydrodynamic diameters ( $d_h$ ) of cMNPs and Gd-doped cMNPs before and after 24 hour exposure of samples to PBS determined by DLS measurements

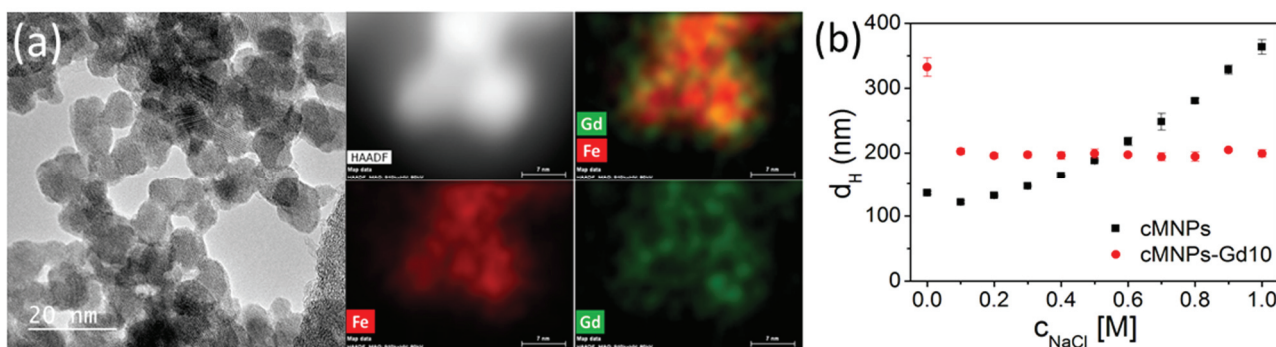


**Figure 4** (a) HRTEM-STEM chemical mapping of cMNPs\_Gd10 and (b) stability (hydrodynamic diameter  $d_h$ ) of cMNPs\_Gd10 in diverse ionic strength.

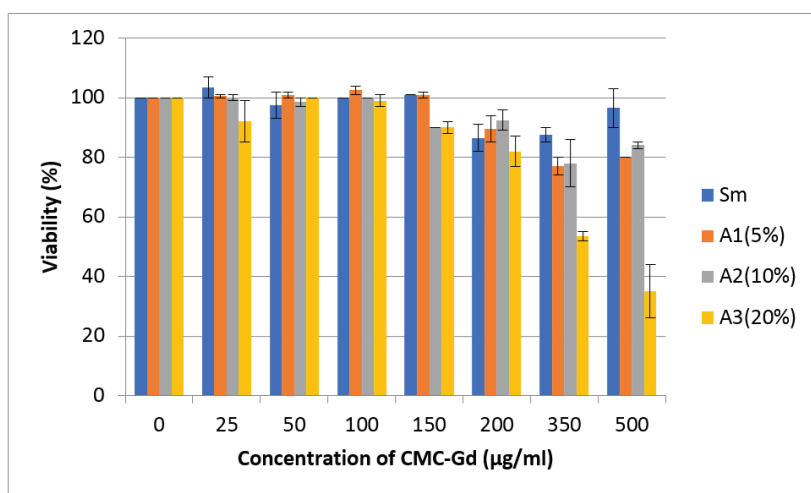


**Figure 5** Viability of NIH3T3 cells after 24 hours of incubation with various cMNPs. Note: Sm (cMNPs), A1 (cMNPs\_Gd5), A2 (cMNPs\_Gd10), A3 (cMNPs\_Gd20). Each error bar represents the average value from three independent measurements

Based on the above mentioned magnetization data, stability and viability results, we realized to perform further biological experiments on cMNPs\_Gd10 sample.

First, we were curious if the labeled stem cells by our cMNPs\_Gd10 can be visible by MRI technique. After 24 hours of incubation with 100  $\mu\text{g/ml}$  NPs  $5 \times 10^5$  of MSCs were collected and centrifugated (see a reddish area in **Figure 6 left**). After that, this pellet of cells was imaged by 1.5 T MRI in T2-weighted images clearly visible as a black sphere in **Figure 6 (right)**. Highly efficient negative contrast effect of labeled MSCs when compared to surrounding medium make the cMNPs\_Gd10 promising candidate for in vivo MSCs monitoring.

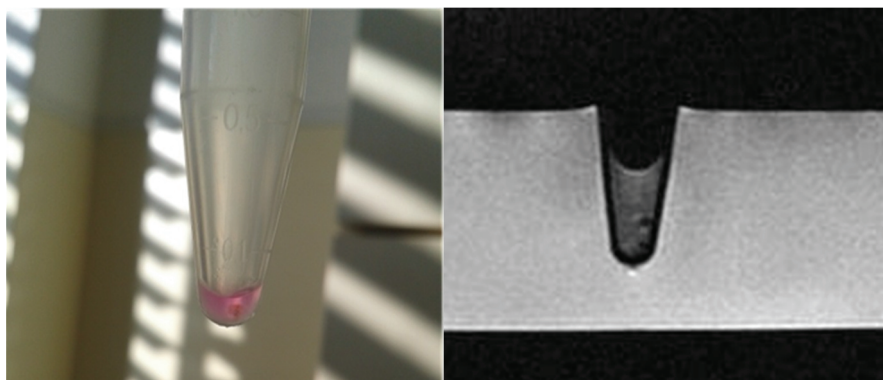


**Figure 6** MRI contrast effect of MSC labeled by cMNPs\_10. (left) reddish pellet of centrifugated labeled MSC, (right) black sphere of the same pellet measured by clinical 1.5 T MRI in T2 weighted images.

One of the important issues of the nanoparticles interacting with cells is their internalization mechanism, localization and degradation within the cells. For this purpose, we covalently bound green fluorescein dye on the surface of cMNPs\_Gd10. After 24 hours, SPIO NPs, most probably internalized by endocytosis, are localized homogenously in the endosomes/lysosomes as green globular areas depicted in **Figure 7 (left)**. Moreover, MNPs are not found in nucleus of cells and cells keep their native morphology and proliferation rate (**Figure 7 left and right**) suggesting their high biocompatibility. Additionally, we can summarize that cMNPs\_Gd10 sample could be used not only for MRI but also for optical imaging which in fact increase the sensitivity of the diagnostics [16].

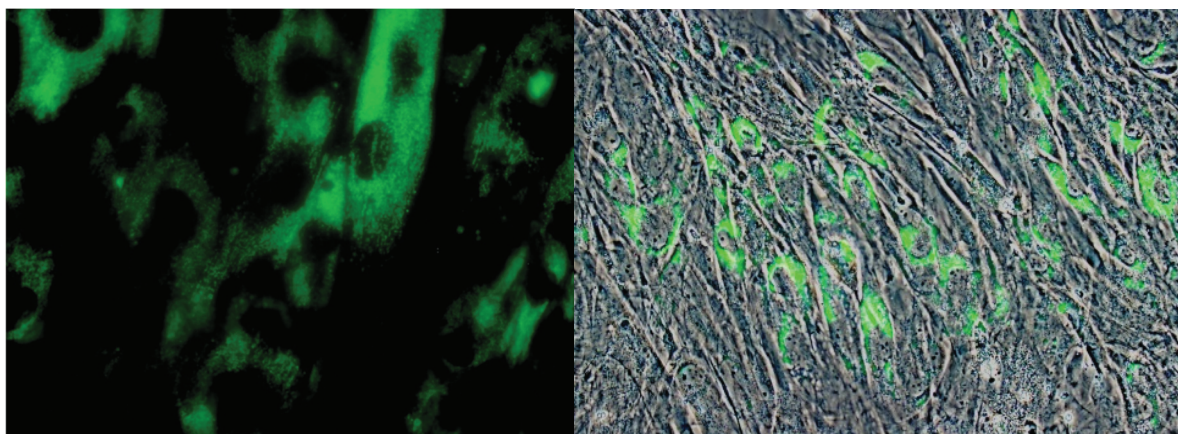


**Figure 7** Localization of cMNPs\_Gd10 nanoparticles in MSCs using optical fluorescence microscopy

## CONCLUSION

In this work, we prepared easily highly stable superparamagnetic iron oxide nanoparticles coated with carboxymethylcellulose polymer containing different amount of chelated Gd. By controlling the amount of Gd

in the synthesis the magnetization properties can be tuned. Moreover, we showed that the most stable cMNPs\_Gd10 bound with fluorescent dye is appropriate for biomedical application as dual contrast agents for MCSs imaging.

## ACKNOWLEDGEMENTS

***The authors acknowledge the support from the Ministry of Education, Youth and Sports of the Czech Republic under Project No. LO1305.***

## REFERENCES

- [1] MEDRIKOVA, Z., NOVOHRADSKY, V., ZAJAC, J. et. al. Enhancing Tumor Cell Response to Chemotherapy through the Targeted Delivery of Platinum Drugs Mediated by Highly Stable, Multifunctional Carboxymethylcellulose-Coated Magnetic Nanoparticles. *Chemistry-A European Journal*. 2016. vol. 22, iss 28, pp 9750-9759.
- [2] WINTER, P. M., CARUTHERS, S. D., WICKLINE, S. A., LANZA, G. M. Molecular Imaging by MRI. *Curr. Cardiol. Rep.* 2006. vol. 8, pp 65-69.
- [3] HU, X., NORRIS, D. G. Advances in High-Field Magnetic Resonance Imaging. *Annu. Rev. Biomed. Eng.* 2004. vol. 6, pp 157-184.
- [4] CHEN, S., ZHANG, Q., HOU Y. et al. Nanomaterials in medicine and pharmaceuticals: nanoscale materials developed with less toxicity. *Eur. J. Nanomed.* 2013. vol. 5.
- [5] SHOKROLLAHI, H. Contrast agents for MRI. *Materials Science and Engineering C*. 2013 vol. 33, pp 4485-4497.
- [6] SKOPALIK, J., POLAKOVA, K., HAVRDOVA, M. et al.; Mesenchymal stromal cell labeling by new uncoated superparamagnetic maghemite nanoparticles in comparison with commercial Resovist - an initial in vitro study. *Int J Nanomed.* 2014, vol. 9, pp 5355-5372.
- [7] LI, L., JIANG, W., LUO, K. et al. Superparamagnetic Iron Oxide Nanoparticles as MRI contrast agents for Non-invasive stem cell labeling and tracking. *Theranostics* 2013, vol. 3, pp 595-615.
- [8] KLUCHOVA, K., ZBORIL, R., TUCEK, J. et. al. Superparamagnetic maghemite nanoparticles from solid-state synthesis - Their functionalization towards peroral MRI contrast agent and magnetic carrier for trypsin immobilization. *Biomaterials* 2009. vol 30, pp 2855-2863.
- [9] POLAKOVA, K., MOCIKOVA, I., PUROVA, D. et al. Magnetic resonance cholangiopancreatography (MRCP) using new negative per-oral contrast agent based on superparamagnetic iron oxide nanoparticles for extrahepatic biliary duct visualization in liver cirrhosis. *Biomed Pap Med Fac Univ Palacky Olomouc Czech Repub.* 2016. vol. 160, pp 512-517.
- [10] MARKOVA, I., POLAKOVA, K., TUCEK, P. et al. MR enterography with a new negative oral contrast solution containing maghemite nanoparticles. *Biomed Pap Med Fac Univ Palacky Olomouc Czech Repub.* 2012, vol. 156, pp 229-235.
- [11] WANG, Y.X., HUSSAIN, S.M., KRESTIN, G.P. et.al. Superparamagnetic iron oxide contrast agents: physicochemical characteristics and applications in MR imaging. *Eur. Radiol.* 2001. vol. 11, pp 2319-2331.
- [12] GUPTA, A.K. and GUPTA, M. Synthesis and surface engineering of iron oxide nanoparticles for biomedical applications. *Biomaterials* 2005. vol. 26, pp 3995-4021.
- [13] BULTE, J.W.M. and KRAITCHMAN, D.L. Iron oxide MR contrast agents for molecular and cellular imaging. *NMR in Biomedicine* 2004. vol. 17, pp 484-499.
- [14] LAURENT, S., FORGE M., PORT, A. et.al. Magnetic Iron Oxide Nanoparticles: Synthesis, Stabilization, Vectorization, Physicochemical Characterizations, and Biological Applications. *Chem. Rev.* 2008. vol. 108, pp 2064-2110.
- [15] CORNELL, R.M. and U. SCHWERTMANN, U. *The Iron Oxides*, 2nd Edition (Wiley-VCH). 2003.
- [16] CMIEL, V., SKOPALIK, J., POLAKOVA, K. et al.; Rhodamine bound maghemite as a long-term dual imaging nanoprobe of adipose tissue-derived mesenchymal stromal cells, *Eur. Biophys. J.* 2017. vol. 46, pp 433-444.